THE JOURNAL OF BIOLOGICAL CHEMISTRY VOL. 280, NO. 51, pp. 42391–42396, December 23, 2005

Novel Conformational States of Peptide Deformylase from Pathogenic Bacterium *Leptospira interrogans*

*IMPLICATIONS FOR POPULATION SHIFT**

Received for publication, June 10, 2005, and in revised form, October 20, 2005 Published, JBC Papers in Press, October 20, 2005, DOI 10.1074/jbc.M506370200

Zhaocai Zhou[‡§], Xiaomin Song[‡§], and Weimin Gong[‡§1]

From the [‡]National Key Laboratory of Biomacromolecules, Institute of Biophysics, Chinese Academy of Sciences, Beijing 100101, People's Republic of China and [§]School of Life Sciences, University of Science and Technology of China, Hefei, Anhui 230026, People's Republic of China

Peptide deformylase is an attractive target for developing novel antibiotics. Previous studies at pH 3.0 showed peptide deformylase from *Leptospira interrogans* (LiPDF) exists as a dimer in which one monomer is in a closed form and the other is in an open form, with different conformations of the CD-loop controlling the entrance to the active pocket. Here we present structures of LiPDF at its active pH range. LiPDF forms a similar dimer at pH values 6.5–8.0 as it does at pH 3.0. Interestingly, both of the monomers are almost in the same closed form as that observed at pH 3.0. However, when the enzyme is complexed with the natural inhibitor actinotin, the conformation of the CD-loop is half-open. Two pairs of Arg^{109}-mediated cation-π interactions, as well as hydrogen bonds, have been identified to stabilize the different CD-loop conformations. These results indicate that LiPDF may be found in different structural states, a feature that has never before been observed in the peptide deformylase family. Based on our results, a novel substrate binding model, featured by an equilibrium between the closed and the open forms, is proposed. Our results present crystallographic evidence supporting population shift theory, which is distinguished from the conventional lock-and-key or induced-fit models. These results not only facilitate the development of peptide deformylase-targeted drugs but also provide structural insights into the mechanism of an unusual type of protein binding event.

Peptide deformylase (PDF),[2] a known essential bacterial metalloenzyme, is responsible for the removal of the *N*-formyl group from the N-terminal methionine of nascent polypeptides (1–4). This process is required for bacterial survival, because mature proteins do not retain *N*-formyl-methionine, and all known N-terminal peptidases cannot utilize formylated peptides as substrate. Eukaryotic cytosolic protein synthesis, however, does not involve deformylase activity. Thus, inhibition of PDF would halt bacterial growth and spare host cell function. In fact, PDF has represented one of the most promising bacterial targets in the search for a novel mode of action antibiotics that lack cross-resistance to existing drugs (5–7). Peptide deformylase inhibitors appear to be one of the most promising classes of antibacterial agents discovered to date. As a metalloprotease, the high degree of structure-function conservation makes rapid progress possible in the development of peptide deformylase inhibitors. Very recently, a new peptide deformylase inhibitor of clinical importance (LBM415) has been characterized (8). Moreover, a new human peptide deformylase (HsPDF) has been suggested to be involved in the deformylation and processing of mitochondrially encoded proteins and may provide a novel selective target for anticancer therapy based on the observation that inhibition of human peptide deformylase (HsPDF) by actinonin (a naturally occurring competitive inhibitor of PDF) also inhibits the proliferation of 16 human cancer cell lines (9).

As a ubiquitous pathogenic bacterium, *Leptospira* can cause strong leptospirosis infection of animals (including humans) by entering the host through mucosa and broken skin. The resultant bacteremia, for example, is frequently found as a post-operative complication. Our previous study about peptide deformylase from *Leptospira interrogans* (LiPDF) revealed some unusual characteristics for the crystal structure obtained at pH 3.0, where no activity is detected (10). Structure comparison suggests LiPDF may represent a new type of PDF, belonging to neither type I nor type II PDFs. As the only dimeric PDF reported so far, the substrate pocket adopts distinct conformations (closed and open) in the two monomers. The primary difference between these two conformations is the structure adopted by a flexible loop (CD-loop, residue 65–76 of LiPDF), which controls access of substrate to the active site of the enzyme. Part of the C-terminal peptide from a symmetry-related molecule is bound to the active site in the open conformation, which was suggested as a mimic of substrate binding (not interacting with an active metal ion). In contrast, access of substrate to the active site is totally blocked in the closed conformation. However, what the conformation is at the active pH (6.5–8.0) and whether the conformational change is triggered by crystal packing remain unknown. Here we present five LiPDF crystal structures (resolutions from 2.3 to 3.1 Å) determined under different conditions. The existence of the closed conformation has been confirmed within the active pH range, with its binding cleft slightly enlarged. Specific interactions between the CD-loop and nearby residues of binding cleft are observed to stabilize the closed conformation. Meanwhile a novel half-open conformation, which has not been observed previously, is defined in the structure of LiPDF bound to an inhibitor molecule actinonin. The CD-loop and Arg^{109} have been repositioned in this new conformation to accommodate the bound actinonin. Based on the three conformational states of LiPDF, an inhibitor binding model has been proposed to include a pre-existing equilibrium and a population shift. This may extend the insights into PDF inhibition,

* This work was supported by the Foundation for Authors of National Excellent Doctoral Dissertation of the Peoples Republic of China (Project 200128), National Foundation of Talent Youth (Grant 30225015), the 973 programs (Grants 2004CB720000 and 2004CB520801), the 863 Special Program of China (Grant 2002BA711A13), the Key Important Project and other projects from the National Natural Science Foundation of China (Grants 10490913, 30121001, and 30130080), and the Chinese Academy of Sciences (KSCX2-SW-224).

The atomic coordinates and structure factors (codes 1VEV, 1VEY, 1SV2, 1VEZ, and 1SZZ) have been deposited in the Protein Data Bank, Research Collaboratory for Structural Bioinformatics, Rutgers University, New Brunswick, NJ (http://www.rcsb.org/).

[1] To whom correspondence should be addressed: Institute of Biophysics, 15 Datun Rd., Chaoyang District, Beijing 100101, P.R. of China. Tel.: 86-10-64888467; Fax: 86-10-64888513; E-mail: wgong@sun5.ibp.ac.cn.

[2] The abbreviations used are: PDF, peptide deformylase; LiPDF, peptide deformylase from *Leptospira interrogans*; MES, 4-morpholineethanesulfonic acid; DDT, 1,1,1-trichloro-2,2-bis(*p*-chlorophenyl)ethane.

TABLE ONE

Data collection and refinement statistics

PDB code	1 VEV	1 VEY	1 SV2	1 VEZ	1 SZZ (inhibitor complex)
pH value	6.5	7.0	7.5	8.0	7.5
Space group	$P4_12_12$	$P4_12_12$	$P4_12_12$	$P4_12_12$	$P2_1$
Cell parameters	$a = b = 82.2$, $c = 201.0$ Å	$a = b = 82.0$, $c = 199.2$ Å	$a = b = 81.5$, $c = 201.6$ Å	$a = b = 83.9$, $c = 204.4$ Å	$a = 87.5$ $b = 119.1$, $c = 95.8$ Å, $\beta = 111.8°$
Resolution (Å)	100–2.5	20–2.9	100–2.3	20–3.0	20–3.1
Total reflections	390,867	245,112	242,753	58,810	183,806
Unique reflection	22,720	14,854	30,947	13,456	31,226
Completeness (last shell) (%)	93.3 (95.4)	93.3 (86.8)	99.2 (99.9)	87.7 (85.2)	94.1 (93.0)
R_{sym}[a]	0.116	0.121	0.075	0.109	0.249
No. of protein atoms	2,692	2,678	2,737	2,692	10,525
No. of metal atoms	2	2	2	2	8
No. of ligand atoms	6	2	6	2	216
No. of water atoms	135	0	159	65	0
R-value	0.258	0.247	0.214	0.227	0.255
R-free	0.289	0.283	0.247	0.270	0.284
Bond length/angle root-mean square deviation (Å/°)	0.01/1.38	0.01/1.36	0.01/1.28	0.01/1.30	0.01/1.37
Overall B-factor (Å^2)	25.5	25.9	28.5	25.6	25.0

[a] $R_{sym} = R_{merge} = \Sigma_{hkl}\Sigma_j|(I(hkl)_j - \langle I(hkl)\rangle)|/\Sigma_{hkl}\Sigma_j(I(hkl)_j)$, where $I(hkl)_j$ is the jth measurement of the intensity of reflection hkl and $\langle I(hkl)\rangle$ is the mean intensity of reflection hkl.

facilitating novel drug design. The hypothetical model may provide an example for an unusual type of protein binding event.

MATERIALS AND METHODS

LiPDF protein was obtained following previously described procedures (10) and was crystallized using the hanging drop method at 277 K. All conditions for experimentation were similar to those reported previously (10, 11), except the solution buffer was subsequently changed to 50 mM HEPES, pH 7.5, 100 mM HEPES, pH 7.0, and 100 mM MES, pH 6.5, respectively. The co-crystallization of LiPDF and actinonin at pH 7.5 has been described previously (12).

All phases of the native crystals were obtained by molecular replacement with the AMORE software package (13). The structure of LiPDF at pH 3.0 (Protein Data Bank code 1Y6H) was taken as an initial search model. Models were refined with crystallography NMR software (14) and rebuilt using the software package O (15). After rigid body and energy minimization refinements, manual building of the C terminus and CD-loop followed by simulated annealing were carried out, with 2-fold non-crystallographic symmetrical redundancy exploited. A zinc atom and the coordinating ligands, as well as the small molecules (DDT, HEPES, MES) in the S1′ pocket, were incorporated into the model by direct examination of $2F_o - F_c$ maps.

The structure of LiPDF complexed with actinonin was determined to a resolution of 3.1 Å using the molecular replacement method. There were eight molecules in each asymmetric unit. Some side chains from the flexible CD-loop were missing. Nevertheless, thanks to the 8-fold non-crystallographic symmetrical redundancy, all of the main chains of CD-loops, as well as the key residue Tyr^{72}, were clear enough for comparison with the native structure. Statistics are shown in TABLE ONE.

RESULTS

Crystal Structures of Free LiPDF between pH Values 6.5 and 8.0, Unusual Closed Conformation—Because the previous study of both the "closed" and "open" states in crystals of LiPDF was performed at pH 3.0, where the enzyme is inactive (10), it is possible that the structure that was determined for the closed state is not a representative conformation of the free active enzyme. We have therefore determined four crystal structures (see TABLE ONE) of free LiPDF within the pH range 6.5– 8.0, where the enzyme is fully active (16). Surprisingly, all four of these structures adopted the same closed conformation, which was similar to that observed at pH 3.0. Nevertheless, a detailed comparison of the closed cleft at active pH with the one at inactive pH does reveal subtle differences, which could be important for the conformational change required for substrate binding (see "Discussion").

The structure of LiPDF determined at pH 7.5 is representative of those within the active pH range. The crystal of LiPDF at this pH belongs to space group $P4_12_12$, with two molecules/asymmetric unit. Each molecule associates with a symmetry-related molecule through hydrophobic interactions, forming a stable dimer (Fig. 1, *top right*). The structures of the two molecules in the asymmetric unit are highly similar, with a root mean square deviation of 0.125 Å for 171 α carbon atoms. The active site metal is a pentacoordinated zinc ion as we have described previously (10), which is liganded by residues Cys^{102}, His^{143}, His^{148}, and a formate group providing two oxygen atoms. The formate group, which is one of the catalytic products of PDF, comes from the crystallization solution.

Similar to the closed structure observed at pH 3.0 (10), the substrate pocket of all of the structures within the active pH range was fully covered by the extended CD-loop, especially by Arg^{71} and Tyr^{72}. (Note that the CD-loop is not involved in crystal packing.) These two bulk residues strongly interacted (cation-π and hydrogen bonding) with the side chain of Arg^{109}, which is on the opposite side of the binding cleft (Fig. 1*A*). As such, in all of these closed structures, the substrate entrance to the catalytic site was blocked. The specific conformation of the CD-loop was highly stabilized by anchoring at three points (N terminus, C terminus, and middle tip), which appears to account for the predominance of this state in free enzyme. One hydrogen bond between the Asn^{69} side chain and the Glu^{46} carbonyl oxygen and another between the Glu^{70} main chain nitrogen and the Glu^{46} side chain formed the N terminus anchor. The middle tip anchor included the cation-π interaction between Tyr^{72} and Arg^{109} and the hydrogen bond between the Arg^{109} side chain and the Arg^{71} carbonyl oxygen. On the C-terminal

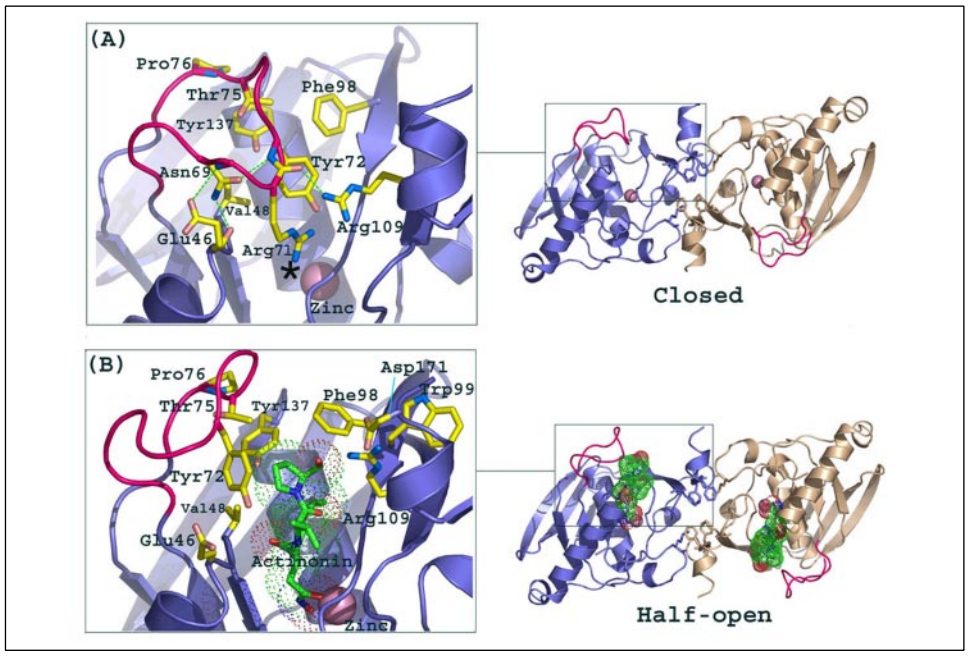

FIGURE 1. **Closed and half-open states of LiPDF.** *A*, the closed state within the active pH range represented by the structure determined at pH 7.5. *B*, the half-open state bound with actinonin. Shown on the *right halves* of both *A* and *B*, dimer is formed through hydrophobic interactions (Phe^{164}, Phe^{166}, Met^{108}, and Met^{9} shown in *stick* model) between two subunits colored in *blue* and *brown*, respectively. Shown on the *left halves* of *A* and *B* are close-up pictures for the closed and half-open pockets, respectively (viewed from same direction). The CD-loop (residue 65–76) is *highlighted* in *red*, and the active zinc ion is in *pink*. In the closed state (*A*), the substrate pocket is blocked and hydrogen bonds are shown by a *green dashed line*. For clarity, the formate group is shown as a *star*. In the half-open state (*B*), the bound competitive inhibitor actinonin is shown in *stick-and-dots* model. In this state, Arg^{71} is completely solvent-exposed and thus disordered. This figure and Fig. 3 were prepared using Pymol.

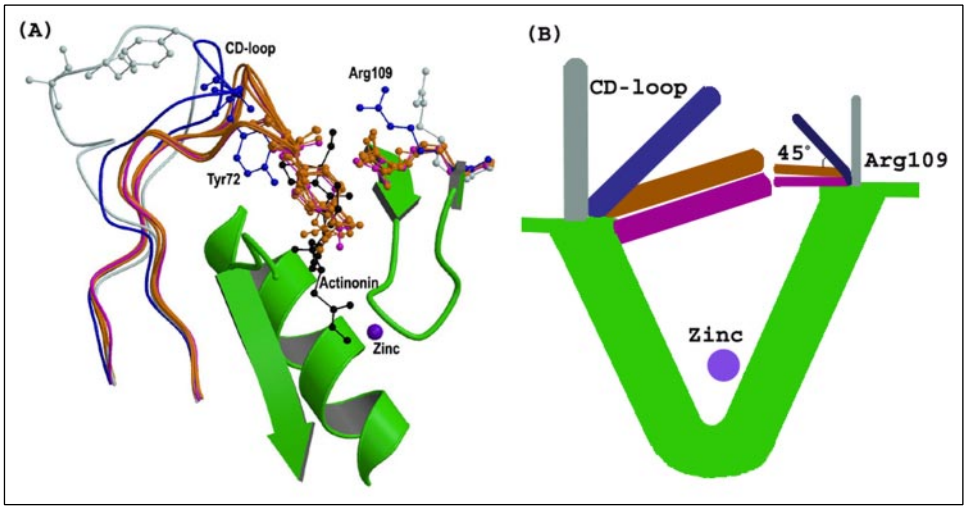

FIGURE 2. **Superposition of all LiPDF structures.** *A*, all observed conformational states of LiPDF are superimposed to reveal the differences around the substrate pocket. *Pink*, closed state at pH 3.0; *brown*, all closed states within pH values 6.5–8.0; *blue*, half-open state; *cyan*, open state at pH 3.0. Residues Tyr^{72} and Arg^{109} (*ball-and-stick* model) undergo significant conformational change during the conversion between different states. The competitive inhibitor actinonin (*black*), which was bound to the half-open state (*blue*) would collide with the pocket in the closed states. With the opening of the substrate pocket, the side chain of Arg^{109} swung up toward the molecular surface. Compared with the closed state at pH 3.0, the closed states within the pH range 6.5–8.0 displayed a slightly open pocket. *B*, a schematic is shown to help compare these different states. The color scheme is consistent in both panels. This figure was prepared using Molscript (30) and Raster3D (31).

end of the CD-loop, the hydrophobic packing of residues Pro^{76}, Thr^{75}, Phe^{98}, and Tyr^{137} provides the third anchor.

Despite the high similarity between closed structures from the active pH and from the inactive pH, the subtle differences observed around the CD-loop anchoring could be significant for the conformational change between the closed and open states. Compared with the structure at pH 3.0, a slightly open substrate binding cleft was observed under active pH (Fig. 2*B*). In the middle tip anchor for the CD-loop, the hydrogen bonding between the Arg^{109} side chain and Arg^{71} carbonyl oxygen was weakened, whereas the cation-π interaction between Tyr^{72} and Arg^{109} became stronger (TABLE TWO). This comparison suggests that the middle tip anchoring is flexible and susceptible to environmental factors, such as pH and ionic strength.

Crystal Structure of the LiPDF-Inhibitor Complex, Novel Half-open Conformation—Because what we observed in the active pH range was a closed conformation that blocks the substrate entrance, the structure of the complex of LiPDF with its competitive inhibitor actinonin was then determined (to 3.1 Å resolution at pH 7.5) to examine its substrate binding ability and catalytic activity on the molecular level.

In the crystal of the LiPDF-actinonin complex, each asymmetric unit contained eight PDF molecules organized as four dimers. The structures of all eight molecules were nearly identical with variations observed in the flexible CD-loop region and the side chain of Arg^{109}. As expected, one actinonin is observed in the substrate pocket of each PDF molecule. The zinc-coordinating formate group in the free LiPDF structure was then replaced with two oxygen atoms of the bound actinonin.

The overall structures of the LiPDF in the actinonin-bound and free states were similar, except the marked conformational change of the CD-loop. A "half-open" conformation was observed, where the actinonin was intimately bound (Fig. 1*B*, *right*). Relative to the closed state, the CD-loop was repositioned with its top end swung outward from the binding cleft by ~6 Å (Fig. 1). Due to the large displacement of the N-terminal and middle part of the CD-loop, stabilizing interactions at this region observed in the closed state did not exist in the half-open state. However, as a result of conformational adjustment, new hydrophobic interactions were formed between the residue Tyr^{72} at the top end of the CD-loop and P3′ Pro and P2′ Val of the bound actinonin. In contrast, for the C-terminal part of CD-loop, the hydrophobic stacking

TABLE TWO

Statistics of Arg-involved cation-π interactions

This calculation was performed according to the systematic method described in Ref. 29. Etotal indicates the strength of the cation-π interaction. According to this method, the candidate interacting pair is considered to be energetically significant only when Etotal < -2.0 kcal/mol.

PDB code	pH	Interacting pairs		E(es)	E(vdw)	Etotal	Conformational substate
		Cation	Pi				
				kcal/mol	*kcal/mol*	*kcal/mol*	
1Y6H(A)	3.0	Arg^{109}	Trp^{99}	−1.78	−1.09	−2.87	Open
1Y6H(B)	3.0	Arg^{109}	Tyr^{72}	−2.04	−2.08	−4.12	Closed
1VEV	6.5	Arg^{109}	Tyr^{72}	−1.93	−2.54	−4.47	Closed
1VEY	7.0	Arg^{109}	Tyr^{72}	−1.83	−2.69	−4.52	Closed
1SV2	7.5	Arg^{109}	Tyr^{72}	−2.34	−2.45	−4.79	Closed
1VEZ	8.0	Arg^{109}	Tyr^{72}	−1.72	−3.13	−4.85	Closed
1SZZ	7.5	Arg^{109}	Trp^{99}	−2.03	−1.09	−3.12	Half-open

of Pro^{76} and Thr^{75} with Tyr^{137} and Phe^{98} was preserved due to the synchronous outward movement of these four residues. Another impressive feature of the half-open conformation was the "swing up" of the Arg^{109} side chain (rotating the $\chi 1$ angle ~45°) from the previous horizontal orientation (Figs. 1 and 2). There the side chain of Arg^{109} formed a salt bridge with Asp^{171} from the C-terminal tail helix, as well as a cation-π interaction with Trp^{99}. The unique topology and positioning of LiPDF C terminus seemed to be required for the interaction between Arg^{109} and Asp^{171}.

Although the binding cleft in this novel conformation was significantly splayed compared with that of the closed structure, it was still much narrower than that of any other PDF where the substrate pocket remained fully open prior to and following inhibitor/substrate binding. Therefore it was not surprising that such a compact binding pocket did not even allow clear access for actinonin without conformational change (see more under "Discussion"). Comparison of this half-open structure with all of the available inhibitor complexes of PDFs revealed a highly conserved inhibitor binding mode. However, additional hydrophobic interaction between Tyr^{72} of the CD-loop and P3′ Pro of actinonin was observed only in the half-open conformation of LiPDF.

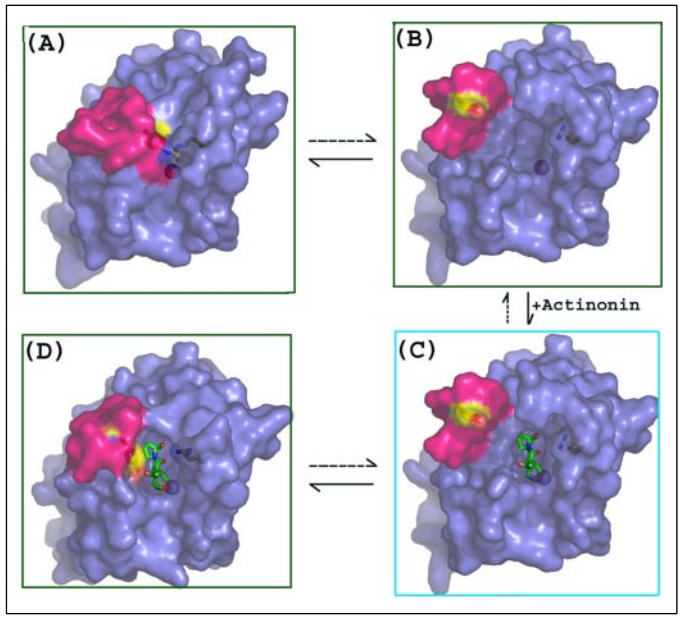

FIGURE 3. **Hypothetical substrate/inhibitor binding model.** *A*, the closed state, as the predominant state in the absence of substrate, cannot bind substrate directly, but has been repeatedly observed at active and inactive pH values with slight differences in the pocket. *B*, the open state was captured at pH 3.0, in which part of the C-terminal peptide (not shown) from a symmetry-related molecule was bound (10). *C*, the open state with actinonin bound was modeled by superimposing the half-open to the open structure. *D*, the half-open state with actinonin bound did not allow free docking of the actinonin. The proposed pre-existing equilibrium (a probable distribution) exists among the closed state (*A*) and all other possible states including the open state (*B*). As an active species, the open state is suggested to be a minor population in the absence of substrate because of its instability without the bound peptide. Thus the pre-existing equilibrium is strongly biased toward the closed state. The selective binding of actinonin to the open state (*B* to *C*) can change the probable distribution of the conformational ensemble. The subsequent induced closing of the pocket (*C* to *D*) results in a stable half-open state. Therefore, via the open state, the major population is shifted from the closed to the half-open. The CD-loop and the rest of the enzyme are shown in *red* and *blue*, respectively. Tyr^{72} and Arg^{109} are shown in *stick* model. The phenyl ring of Tyr^{72} is *highlighted* in *yellow*. The actinonin is depicted as a *green stick*. The *small sphere* represents the active zinc ion.

DISCUSSION

Three Conformational States of LiPDF—Our previous study of LiPDF at pH 3.0 (10) revealed a non-free open conformation and a free closed conformation. The open conformation, as a peculiar artifact of crystallization, resulted from the binding of the C terminus peptide of a symmetry-related molecule. Coincidentally, the N terminus of a symmetry-related molecule was also observed in the substrate pocket of the peptide deformylase from *Staphylococcus aureus*, which was suggested to mimic substrate binding (17). Thus the open conformation of LiPDF may resemble the state where actual substrate is bound. However, the CD-loop in this state was specifically stabilized by the interaction between Tyr^{72} and the bound peptide (10). Removal of the bound peptide would result in a completely solvent-exposed and hence highly unstable CD-loop. All structures of LiPDF indeed adopted a closed (but not open) conformation in the free state. Actinonin could freely dock into the substrate pocket of the open state when bound peptide was removed (Fig. 3*C*).

The existence of the closed conformational state is now confirmed at the active pH range. Both monomers in the asymmetric unit showed the same closed conformation, even though they faced a different environment in the crystal. Nevertheless, here the closed form of free LiPDF possibly describes a state that was ready to open its binding cleft. Furthermore, the recurrence of the stable closed state for free LiPDF in different conditions suggests that such a conformation would also occur in solution and would predominate in the absence of substrate/inhibitor. On the other hand, the side chain of Tyr^{72} would collide with the side chains from P2′ and P3′ when the inhibitor actinonin is modeled into the closed substrate pocket. This clearly indicates that the active site in the closed state of free LiPDF is not accessible when no conformational changes occur.

The current structure of the complex substantiates the substrate binding ability as well as the catalytic activity of LiPDF, in keeping with our previous biochemical studies (16). Here a novel conformation was

observed as half-open, instead of fully open. Crystal-packing examination also revealed that the CD-loop region is essentially solvent-exposed in all of the eight molecules. In this half-open state, the actinonin molecule was snugly bound in the active crevice. In contrast to studies of PDFs from different species, where P3′ proline of the bound actinonin is solvent-exposed (18–19), in LiPDF, the P3′ proline of the bound actinonin was partially covered by a hydrophobic environment due to the special positioning of the CD-loop. This hydrophobic S3′ subsite consisted of Tyr^{72} and Thr^{75} from the CD-loop and the adjacent residues Tyr^{137}, Phe^{98}, and Val^{48}. A detailed examination of the binding cleft revealed an unexpectedly confined entrance. Although the close interaction between Tyr^{72} and Arg^{109} did not exist, their side chains are still within a distance of 6 Å. Here it is worth noting that the half-open cleft of the enzyme trapped the bound actinonin. A free docking or release (no close contact with a distance of $<$1.5Å between actinonin and enzyme) of actinonin into the half-open state therefore requires a conformational change to take place. Thus it can be safely inferred that the present half-open state is an induced outcome from a more open state where actinonin can freely dock.

In summary, three distinct conformational states of LiPDF (open, closed, and half-open) have now been identified. At this stage, these states have not been assigned to the inhibitor binding mechanism. However, our cation-π interaction analysis for all of these states identified two energetically significant pairs, both of which involve Arg^{109} (Fig. 1 and TABLE TWO). One was formed between Arg^{109} and Tyr^{72}, observed only in the closed state. Another was formed between Arg^{109} and the pocket rim residue Trp^{99}, observed only in the half-open or open states. In keeping with the cation-π interaction, the hydrogen bond between Arg^{109} and Arg^{71} only existed in the closed state, and the salt bridge between Arg^{109} and Asp^{171} only existed in the half-open or open states. In the closed state, the Arg^{109}-related cation-π interaction and hydrogen bonding formed a bridge across the active pocket. In the half-open or open state, because Arg^{109} and Trp^{99} were on the same side of the binding cleft, the cation-π interaction between them, together with the salt bridge between Arg^{109} and Asp^{171}, helped to keep the specific conformation of the Arg^{109} side chain after the CD-loop was released from the Arg^{109}-mediated bridge. Therefore Arg^{109} appears to be a pivotal residue for the conformational changes triggered by substrate binding. Note that Arg^{109} structurally corresponds to residue Arg^{97} in peptide deformylase from *Escherichia coli* (20).

Hypothetical Model for Substrate Binding—Traditionally, conformational changes related to protein binding events have been described by lock-and-key or induced-fit models. However, these two models do not fit the case of LiPDF, because the free enzyme was observed to be in a closed form, and no inducer molecule has been found for LiPDF or for other PDFs.

As an alternative, the pre-existing equilibrium hypothesis (21) is based on protein folding and conformational selection theories of the funnel energy landscape (22–25), which postulates that the native state of a protein contains an ensemble of conformations at its binding site, rather than a unique fold. In this view, the energy landscape of the protein is dynamic, changing with environmental factors such as pH, ionic strength, and the presence of other molecules. The most populated conformation of a protein may be different prior to and following a binding event, corresponding to a change in the energy landscape. A ligand will bind selectively to an active conformation, thereby biasing the equilibrium toward the binding conformation. An elegant example comes from the study of a monoclonal IgE antibody, SPE7, in which both x-ray crystallography and presteady-state kinetics revealed an equilibrium between at least two different pre-existing isomers (binding structurally distinct antigens) that can both be crystallized in the absence of any ligand (26).

Based on this theory and our observations, we suggest that the closed state of free LiPDF might not be the only conformation adopted in solution. Instead, the open form of LiPDF may co-exist with the closed form, although as the minor population. Because the crystallization process may select one of the populations to form a crystal, but not necessarily the "active" conformers, the three conformational states imply a hypothetical model for substrate binding in LiPDF (Fig. 3). For the free enzyme, a strong, biased equilibrium between closed and open states is suggested, as above. The substrate binding would trigger a redistribution of the closed and open states in the ensemble of conformations. After an initial binding to the open state, the substrate pocket is then induced to shut, leading to the final half-open conformation, as observed in the complex. In this model, we suggest that the pivotal residue Arg^{109}, which is on molecular surface, could be sensitive to the environmental disturbances; therefore the locking bridge (mainly contributed by the interactions between Arg^{109} and the CD-loop) could be momentarily broken, leading to a conformational ensemble. Among these conformations, the predominant closed state is thermodynamically favored in the absence of ligand, whereas other minor states (including the observed half-open and open states from non-free enzyme) would have a low population time. However, in the presence of substrate, tight binding to the active site stabilizes the open sate. At the final stage, the hydrophobic interactions between Tyr^{72} and the substrate (especially proline at P3′ and valine at P2′) possibly induce the repositioning of the CD-loop and result in the half-open state.

Conclusion and Perspective—As a novel drug design target from a real pathogen, LiPDF showed unique structural features highlighted by its three conformational states. A pre-existing equilibrium-based model has been proposed for the competitive inhibitor binding. Besides providing structural information for drug development, this model may extend our insights into an unusual type of enzymatic binding event.

Meanwhile, we have noticed that the structures of deformylase from other bacteria do not show significant conformational changes upon inhibitor binding. This suggests that the conformational change observed in LiPDF is not a general feature regarding deformylase activity itself. Why does LiPDF use this machinery? It has been realized that a protein that adopts several different conformations could, in principle, have several different functions (28). Genomics data indicate that many species have two copies of similar but different PDF genes, and PDF genes are also found in eukaryotics. Thus at this stage, we cannot rule out the possibility that peptide deformylase (in at least some species) have additional biological functions besides modifying the newly synthesized peptide.

Acknowledgments—We thank Prof. Peng Liu and Yuhui Dong of the Institute of High Energy Physics for diffraction data collection. Special thanks go to Jerry Brown at Brandeis University for his reading of the manuscript.

REFERENCES

1. Adams, J. M., and Capecchi, M. R. (1966) *Proc. Nat. Acad. Sci. U. S. A.* **55,** 147–155
2. Adams, J. M. (1968) *J. Mol. Biol.* **33,** 571–589
3. Takeda, M., and Webster, R. E. (1968) *Proc. Nat. Acad. Sci. U. S. A.* **60,** 1487–1494
4. Livingston, D. M., and Leder, P. (1969) *Biochemistry* **8,** 435–443
5. Mazel, D., Pocher, S., and Marliere, P. (1994) *EMBO J.* **13,** 914–923
6. Bradshaw, R. A., Brichey, W. W., and Walker, K. W. (1998) *Trends Biochem. Sci.* **23,** 263–267
7. Giglione, C., Pierre, M., and Meinnel, T. (2000) *Mol. Microbiol.* **36,** 1197–1205
8. Fritsche, T. R., Sader, H. S., Cleeland, R., and Jones, R. N. (2005) *Antimicrob. Agents Chemother.* **49,** 1468–1476

9. Lee, M. D., She, Y., Soskis, M. J., Borella, C. P., Gardner, J. R., Hayes, P. A., Dy, B. M., Heaney, M. L., Philips, M. R., Bornmann, W. G., Sirotnak, F. M., and Scheinberg, D. A. (2004) *J. Clin. Investig.* **114,** 1107–1116
10. Zhou, Z., Song, X., Li, Y., and Gong, W. (2004) *J. Mol. Biol.* **339,** 207–215
11. Li, Y., Ren, X., and Gong, W. (2001) *Acta Crystallogr. Sect. D* **58,** 846–848
12. Zhou, Z., and Gong, W. (2004) *Acta Crystallogr. Sect. D* **60,** 137–139
13. Navaza, J. (1994) *Acta Crystallogr. Sect. A* **50,** 157–163
14. Brunger, A. T., Adams, P. D., Clore, G. M., DeLano, W. L., Gros, P., Grosse-Kunstleve, R. W., Jiang, J. S., Kuszewski, J., Nilges, M., Pannu, N. S., Read, R. J., Rice, L. M., Simonson, T., and Warren, G. L. (1998) *Acta Crystallogr. Sect. D* **54,** 905–921
15. Jones, T. A., Zou, J. Y., Cowan, S. W., and Kjeldgaard, M. (1991) *Acta Crystallogr. Sect. A* **47,** 110–119
16. Li, Y., Chen, Z., and Gong, W. (2002) *Biochem. Biophys. Res. Commun.* **295,** 884–889
17. Kreusch, A., Spraggon, G., Lee, C. C., Klock, H., McMullan, D., Ng, K., Shin, T., Vincent, J., Warner, I., Ericson, C., and Lesley, S. A. (2003) *J. Mol. Biol.* **330,** 309–321
18. Hao, B., Gong, W., Rajagopalan, P. T., Zhou, Y., Pei, D., and Chan, M. K. (1999) *Biochemistry* **38,** 4712–4719
19. Guilloteau, J. P., Mathieu, M., Giglione, C., Blanc, V., Dupuy, A., and Chevrier, M. (2002) *J. Mol. Biol.* **320,** 951–962
20. Chan, M. K., Gong, W., Rajagopalan, P. T., Hao, B., Tsai, C. M., and Pei, D. (1997) *Biochemistry* **36,** 13904–13909
21. Tsai, C. J., Kumar, S., Ma, B., and Nussinov, R. (1999) *Protein Sci.* **8,** 1181–1190
22. Frauenfelder, H., Sligar, S. G., and Wolynes, P. G. (1991) *Science* **254,** 1598–1603
23. Dill, K. A., and Chan, H. S. (1997) *Nat. Struct. Biol.* **4,** 10–19
24. Feher, V. A., and Cavanagh, J. (1999) *Nature* **400,** 289–293
25. Fereire, E. (1999) *Proc. Nat. Acad. Sci. U. S. A.* **96,** 10118–10122
26. James, L. C., Roversi, P., and Tawfik, D. S. (2003) *Science* **299,** 1362–1367
27. Deleted in proof
28. Ma, B., Shatsky, M., Wolfson, H. J., and Nussinov, R. (2002) *Protein. Sci.* **11,** 84–197
29. Gallivan, J. P., and Dougherty, D. A. (1999) *Proc. Nat. Acad Sci. U. S. A.* **96,** 9459–9464
30. Kraulis, P. (1991) *J. Appl. Crystallogr.* **24,** 946–950
31. Merritt, E. A., and Bacon, D. J. (1997) *Methods Enzymol.* **277,** 505–524